CASTRO-ORGAZ, O., and CHANSON, H. (2014). "Depth-Averaged Specific Energy in Open-Channel Flow and Analytical Solution for Critical Irrotational Flow over Weirs." *Journal of Irrigation and Drainage Engineering*, ASCE, Vol. 140, No. 1, Paper 04013006, 8 pages (DOI: 10.1061/(ASCE)IR.1943-4774.0000666) (ISSN 0733-9437 [Print]; ISSN: 1943-4774 [online]).

Depth-Averaged Specific Energy in Open Channel Flow and Analytical Solution for Critical Irrotational Flow Over Weirs

Oscar Castro-Orgaz[1] and Hubert Chanson[2]

Abstract:

Free surface flow in open channel transitions is characterized by distributions of velocity and pressure that deviate from uniform and hydrostatic conditions respectively. Under such circumstances the widely used expressions in textbooks [e.g. $E=h+U^2/(2g)$ and $h_c=(q^2/g)^{1/3}$] are not valid to investigate the changes in velocity and depth. A depth-averaged form of the Bernoulli equation for ideal fluid flows introduces correction coefficients to account for the real velocity and pressure distributions into the specific energy equation. The behavior of these coefficients in curvilinear motion at and in the neighbourhood of control sections was not documented in the literature. Herein detailed two-dimensional ideal fluid flow computations are used to characterize the entire velocity and pressure fields in typical channel controls involving transcritical flow, namely the round-crested weir, the transition from mild to steep slope and the free overfall. The detailed two-dimensional ideal fluid flow solution is used to study the behavior of the depth-averaged coefficients, and a novel generalized specific energy diagram is introduced using universal coordinates. The development is used to pursue a simplified critical flow theory for curved flow, relevant to water discharge measurements with circular weirs.

DOI: 10.1061/(ASCE)IR.1943-4774.0000666

CE Database subject headings: Critical flow conditions, Ideal fluid flow theory, Open channels, Water discharge measurement, Weirs

---

[1]Research Hydraulic Engineer, Instituto de Agricultura Sostenible, CSIC, apdo 4084, Alameda del Obispo s/n, 14080, Cordoba, Spain. E-mail: oscarcastro@ias.csic.es

[2] Professor in Hydraulic Engineering, The University of Queensland, School of Civil Engineering, Brisbane QLD 4072, Australia. Email: h.chanson@uq.edu.au.

Introduction

Transcritical flow in open channels involves distributions of velocity and pressure that deviates from uniform and hydrostatic conditions, respectively (Montes 1998, Chanson 2006). Typical cases are the flow over a round-crested weir or a free overfall, where the flow curvature induces centrifugal force effects that results in a non-hydrostatic pressure and non-uniform velocity (Jaeger 1956, Vallentine 1969). The 'specific energy equation' (Bakhmeteff 1932a) is a widely used tool in hydraulic engineering, although it is based on the assumptions of a uniform velocity and hydrostatic pressure distributions:

$$E = h + \frac{U^2}{2g} \qquad (1)$$

where E=specific energy, h=flow depth, U=mean flow velocity=q/h, q= discharge per unit width and g=gravity acceleration. The underlying assumptions behind Equation (1) imply that the 'specific energy equation' [Eq. (1)] is not valid to study the flow in open channel transitions. However, the 'specific energy equation' is commonly used to explain, qualitatively, the changes of flow depth and velocity in smooth transitions where friction can be neglected. For example, Henderson (1966) used a differential form of Equation (1) to explain the flow over the round-crested weir, and Rouse (1938) used Equation (1) to describe changes in velocity and depth in a channel step. This is a contradiction, because of in both flow problems the pressure is not hydrostatic, the velocity non-uniform and Equation (1) can not yield any realistic prediction of velocity or depth. Rouse (1932) made a worthy documentation of the two-dimensional flow behavior of channel flow in short transitions using model testing, i.e. the transition from mild to steep slope and the free overfall. It appears, therefore, that either model testing or full two dimensional (2D) ideal fluid flow simulations (Vallentine 1969) are required to obtain the accurate picture of flow in a channel transition. Jaeger (1956) advocated the introduction of velocity and pressure correction coefficients in the one dimensional specific energy equation to extend its use to general flows in channel transitions. However, general analytical results were neither presented nor specific evaluation of the correction coefficients using detailed 2D ideal fluid flow computations.

A depth-averaged form of the Bernoulli equation for ideal fluid flows introduces in the specific energy correction coefficients to account for the actual velocity and pressure distributions (Liggett 1993, Chanson 2006). This higher order equation can be used to describe the actual flow changes of velocity and depth with generality. The first objective of this contribution is to study the behavior of the depth-averaged coefficients in curvilinear motion at and in the neighborhood of control section using detailed two-dimensional ideal fluid flow computations. This will not provide a catalogue of depth-averaged coeffcients than can be read and then applied to all transitional flow cases. Instead, this will reveal how the general energy equation behaves at channel controls using selected test cases. Thus, the 2D model will permit a generalized view of the 1D flow model in channel transitions This important theoretical information will provide insights that can be used to find simplified forms of the energy equation for practical applications. A new generalized specific energy diagram is introduced using universal coordinates, where the flow in channel transitions can be depicted with complete generality. The contribution presents for the first time the depth-averaged form of two-dimensional fluid flows at channel controls. A simplified critical flow theory for curved flow is proposed, based on the depth-averaged results, for water discharge measurement purposes with circular weirs.

Depth-averaged open channel flow diagram

In open channels flows with arbitrary distributions of velocity and pressure, the depth averaged specific energy is defined as (Rouse 1932, Liggett 1993, Montes 1998, Chanson 2006)

$$E = \frac{1}{h}\int_0^h \left(\frac{p}{\gamma} + y + \frac{u^2 + v^2}{2g} \right) \mathrm{d}y = \Lambda h + \beta \frac{q^2}{2gh^2} \qquad (2)$$

where p=pressure, γ=ρg=specific weight of water, y=elevation, u=horizontal velocity in the x-direction and v=vertical velocity in the y-direction; and the depth-averaged correction coefficients Λ and β are respectively

$$\Lambda = \frac{1}{h^2}\int_0^h \left(\frac{p}{\gamma} + y \right) \mathrm{d}y \qquad (3a)$$

$$\beta = \frac{1}{U^2 h}\int_0^h \left(u^2 + v^2 \right) \mathrm{d}y \qquad (3b)$$

where Λ=piezometric pressure correction coefficient and β=kinetic energy correction coefficient. Equation (2) expresses a depth-averaged specific energy, calculated between streamlines for an incompressible and inviscid fluid (Rouse 1938, Vallentine 1969, Montes 1998).

At spillway crest or a free overfall (Fig. 1), the discharge may be expressed as a function of the upstream head above crest as

$$q = C_d \left(g E_{\min}^3 \right)^{1/2} \qquad (4)$$

where C_d=discharge coefficient and $E_{\min}$=upstream head above crest (or minimum specific energy). The upstream head above crest corresponds to the minimum specific energy for a frictionless fluid. Introducing Equation (4) into Equation (1), it becomes

$$\left(\frac{\Lambda h}{E_{\min}}\right)^2\left(\frac{E}{E_{\min}}\right)-\left(\frac{\Lambda h}{E_{\min}}\right)^3=\frac{\beta C_d^2\Lambda^2}{2} \tag{5}$$

Equation (5) is a generalized channel flow relationship at an arbitrary section in curvilinear flow. At a section of minimum specific energy $E=E_{\min}$, Equation (5) reduces to the equation developed by Chanson (2006). Equation (5) is plotted in Figure 2, where it can be observed the effect of the ratio $E_{\min}/E$. Figure 2 shows the relations between water depth and discharge for a given specific energy when the flow is curvilinear. This type of relationship was first proposed by Bakhmeteff (1932a) for hydrostatic pressure and uniform velocity distributions.

Using Figure 2 the behaviour of curvilinear flows involving minimum specific energy conditions in any part of the flow domain can be investigated if the depth-averaged coefficients are determined. With this information, it is possible to obtain a one-dimensional interpretation of the flow near critical flow sections. To the authors' knowledge, this information has so far not been presented in the literature. Thus, in the next section a full two-dimensional ideal fluid flow numerical solution for flows with minimum specific energy is developed. The depth-averaged coefficients will be determined numerically and the one-dimensional characteristics of the flow investigated.

Numerical solution of two-dimensional ideal fluid flow

Method of solution

The estimate of the correction coefficients Λ and β requires a detailed 2D description of the velocity field (u, v) at any point (x, y) in order to evaluate numerically the integrals given by Equations (3a) and (3b). The computation of the 2D flow field was done solving the equations for an inviscid and irrotational flow. The numerical model is based on a semi-inverse mapping of Laplace equation, described in detail by Montes (1994) and Castro-Orgaz (2013). The semi-inverse mapping or x-ψ method (Montes 1992, 1994) is adequate for open channel flow, where ψ=stream function. Montes proposed to solve the Laplacian for y as a function of the pair of variables (ψ, x). The Laplacian of this semi-inverse transformation y=y(x, ψ) is

$$\frac{\partial^2 y}{\partial x^2}\left(\frac{\partial y}{\partial \psi}\right)^2+\frac{\partial^2 y}{\partial \psi^2}\left[1+\left(\frac{\partial y}{\partial x}\right)^2\right]-2\frac{\partial^2 y}{\partial x \partial \psi}\frac{\partial y}{\partial x}\frac{\partial y}{\partial \psi}=0 \qquad (6)$$

This must be solved subject to suitable boundary conditions. The computation directly yields the equation for each streamline y=y(x, ψ=const), from which the velocity components of the potential flow are obtained. The boundary sections up- and downstream are selected where streamlines are parallel to the channel bottom. Equation (6) was discretized using first order central derivatives and details of the numerical solution can be found elsewhere (Thom and Apelt 1961, Montes 1992, Montes 1994, Castro-Orgaz 2013). Once the velocity profiles are computed from the numerical solution of Equation (6), the pressure distribution is deduced from the Bernoulli equation.

Flow over a round-crested weir

The experimental data of Sivakumaran et al. (1983) for a symmetrical hump of profile y=20exp[−0.5(x/24)^2] (cm) is plotted in Figure 3a. The computed water surface and bed pressure profiles obtained from the 2D ideal fluid flow solution shows excellent agreement with the experimental data, indicating the accuracy of the 2D ideal fluid flow numerical model. The velocity and pressure profiles at 3 representative sections are plotted in Figure 3b. At section x/h_c=−2 the pressure distribution is hydrostatic, as indicated by the coincidence of free surface and bottom pressure profiles in Figure 3a. The u velocity profile is non-uniform, however, and the vertical pressure v is clearly non-zero, as inferred from the notable slope of the weir surface at this section. At the crest section, where E=$E_{\min}$, the pressure distribution is below hydrostatic and the velocity components (u, v) are non-uniform, with typical shapes observed previously (Fawer 1937, Vo

1992). At the section x/h_c=+4 the profiles (u, v) are essentially constant, but the pressure distribution is markedly higher than hydrostatic, given the centrifugal effect on the supercritical flow in the tailwater weir face. The profiles (u, v, p) were generated in the mathematical model at 180 sections with a vertical division given by 20 streamlines. The integrals given by Equations (3a) and (3b) were determined numerically and the results are plotted in Figure 3c. The streamwise evolution of β shows values slightly above unity until the spillway crest. However, it grows rapidly in the supercritical portion of the weir. The maximum value is 1.3 at x/h_c=2.2. Such a relatively high value is associated with the notable vertical velocity component v in the supercritical flow portion. This can be seen in Figure 3c by comparing the results with the momentum correction coefficient β_x (i.e. Boussinesq coefficient) defined as

$$\beta_x = \frac{1}{U^2 h}\int_0^h u^2 \mathrm{d}y \qquad (7)$$

The Boussinesq coefficient is close to unity along the whole computational domain, whereas β is especially high for x/h_c>0. The coefficient Λ decreases from unity (hydrostatic pressure) as the weir crest is approached, reaching a minimum value of 0.77 at x/h_c=1.1 (Fig. 3c). From that section the coefficient increases given the reverse trend in centrifugal effects, reaching a maximum value of 1.33 at x/h_c=4.4. As the tailwater horizontal section of the weir is approached, both β and Λ tend to unity.

The data presented in Figure 3 permits a computation for every channel section x/h_c of the corresponding depth-averaged coordinates of the flow ($\Lambda h/E_{\min}$, $1/2\beta C_d^2\Lambda^2$). Equation (5) is plotted in Figure 4 as a function of $E_{\min}/E$, where the data corresponding to Figure 3 are reported. The crest point perfectly lies on the lower branch of the diagram for $E_{\min}=E$, thereby confirming by two dimensional ideal fluid flow computations that critical flow conditions takes place at this section.

The sections $-6<x/h_c<0$ correspond to subcritical flow motion; shortly before the crest every section lies in the upper part of the diagram corresponding to the particular ratio $E_{\min}/E$. Supercritical flow sections in the domain $0<x/h_c<6$ are seen in the lower part of the depth-averaged diagram for a particular value of $E_{\min}/E$. The points plotted in Figure 4 from the 2D ideal fluid flow data present a complete transcritical flow motion across a control section in curvilinear flow.

Flow in transition from mild to steep slope

Figure 5a presents the experimental data of Hasumi (1931) for a slope transition composed by a horizontal reach followed by a circular-shaped transition profile of R=0.1 m that finishes in a steep slope reach of 45º inclination. The upstream and downstream boundary sections were located at $x/h_c=\pm3$. For frictionless flow $E=E_{\min}=1.5h_c$ is seen for $x/h_c<0$. The computed water surface and bed pressure profiles obtained by ideal fluid flow computations are compared in Figure 5a with the experimental data, indicating in a good agreement. The velocity and pressure profiles at three representative sections are plotted in Figure 5b. At section $x/h_c=-1$ the pressure distribution is close to hydrostatic. At the brink section the pressure distribution is considerably below the hydrostatic line and the velocity components (u, v) are highly non-uniform, in agreement with Montes (1994). At the section $x/h_c=+1$ the vertical velocity magnitude of v is large and of the same order as u. The pressure distribution is close to zero in the major part of this section. The integrals given by Equations (3a) and (3b) were evaluated from the ideal fluid flow data and the numerical results are plotted in Figure 5c. The variation of β shows values slightly above unity until the brink section. For comparison, the variation of the Boussinesq coefficient β_x shows that it is close to unity along the whole computational domain. It may be then concluded that the effect of v in the computation of β is small for the horizontal channel reach. This supports the recent computations of Felder and Chanson (2012), who investigated the velocity and pressure coefficients in horizontal broad-crested weirs. However, there is a sharp increase of β in the chute portion, not investigated by Felder and

Chanson (2012). This effect is due to the vertical velocity component v in the steep channel, linked with the definition of the y-coordinate and the chute bed slope. Note that $U=q/h$ is the average velocity in the x-direction, not parallel to the chute bed (Montes 1994). As previously indicated the magnitude of v is similar to u at section $x/h_c=+1$, for example. Near $x/h_c=3$ results $\beta\approx 2\beta_x\approx 2$, originating from $u\approx v$ and $\beta_x\approx 1$. The maximum value of β is 2.17 at $x/h_c=1.6$. This high value is associated with the notable non-uniform vertical velocity component v in the supercritical flow portion. The coefficient Λ decrease from unity (hydrostatic pressure) as the brink section is approached, reaching a minimum value of 0.177 at $x/h_c=0.6$. From that section the coefficient increases given the partial recovery of pressure, but in the tailwater portion it remains close to 0.75 due to the bottom slope effect.

The data presented in Figure 5 was used to obtain the corresponding depth-averaged coordinates of the flow ($\Lambda h/E_{\min}$, $1/2\beta C_d^2\Lambda^2$). The 2D data is plotted in depth-averaged coordinates in Figure 6. The whole flow profile in the horizontal slope reach is a critical flow, in agreement with the physical study of Felder and Chanson (2012). The brink section is a particular critical flow section where the effects of flow curvature are most pronounced. The flow in the supercritical steep chute follows a similar trend to that observed in the tailwater portion of the weir in Figure 3.

Flow in horizontal free overfall

The numerical model was used to solve the 2D problem of a free overfall in a horizontal smooth channel. The ideal fluid flow results are compared with the measurements by Rouse (1932) in Figure 7a, resulting a good agreement. The velocity and pressure profiles at 3 representative sections are plotted in Figure 7b, and are in agreement with previous results by Montes (1992). The depth-averaged coefficients are depicted in Figure 7c, showing a similar behaviour to the mild to steep transition flow. A particular issue is that the pressure inside the jet ($x/h_c>0$) is close to zero shortly after the brink section, resulting in an asymptotic value for Λ in the jet of 0.5. The 2D ideal fluid flow data is plotted in depth-averaged form in Figure 8. The flow motion is similar to the slope break flow. The horizontal reach flow is a critical flow motion, whereas the free jet behaves essentially as a variable-slope steep chute with zero bottom pressure. The high values of β are associated with the notable vertical velocity component v in the (vertical) y-direction as compared to the depth-averaged velocity U in the x-direction.

Critical depth in curvilinear overflows

Analytical development

In the previous section a full 2D model was applied to channel transitions. It was found that both β and Λ deviates from the standard hydraulic values β=1 and Λ=1. These effects need to be accounted for in practical applications. In irrotational flow the local energy head is a constant for all the streamlines of an ideal fluid flow (Rouse 1938, Vallentine 1969). In this case, the value of E given by Equation (2) may be evaluated by the specific energy of the free surface streamline. This idea was pursued by Bakhmeteff (1932b), who assumed that, at the section of $E_{\min}$ in flow over a spillway crest, the velocity distribution follows a free vortex law. Using this simple approximation, the mathematical expression for β is determined and Λ follows from Bernoulli's relation. The analytical expression for E is (Bakhmeteff 1932b)

$$E = \Lambda h + \beta \frac{q^2}{2gh^2} = h + \Omega^2 \frac{q^2}{2gh^2} \qquad (8)$$

where the curvature correction coefficient Ω is

$$\Omega = \frac{\kappa h}{\left(1+\kappa h\right)\ln\left(1+\kappa h\right)} \qquad (9)$$

CASTRO-ORGAZ, O., and CHANSON, H. (2014). "Depth-Averaged Specific Energy in Open-Channel Flow and Analytical Solution for Critical Irrotational Flow over Weirs." *Journal of Irrigation and Drainage Engineering*, ASCE, Vol. 140, No. 1, Paper 04013006, 8 pages (DOI: 10.1061/(ASCE)IR.1943-4774.0000666) (ISSN 0733-9437 [Print]; ISSN: 1943-4774 [online]).

and κ=1/R is the crest curvature and R is the crest radius. Note that this simple approximation permits to reduce the general form of the energy equation with undetermined (general) coefficients [(Eq.(2)], to a simplified equation that is a function of the local water depth [(Eq.(8)]. This step is of great service for practical purposes, as given R the function E only depends on h, thereby allowing 1D critical flow computations. Dressler (1978) developed curved flow equations accounting for bed curvature by perturbations. Dressler equations for steady flow reduce to the free vortex velocity distribution, and, the steady specific energy equation used by Sivakumaran et al. (1981, 1983) is Equation (8), originally proposed by Bakhmeteff (1932b). Ramamurthy and Vo (1993a) used Dressler vortex flow velocity distribution to find an analytical function for the discharge coefficient C_d in weir flow. This function depends upon the value of $E_{\min}$, h_{crest} (crest overflow depth) and the crest bottom pressure. Thus, an evaluation of C_d using this proposal requires estimation of these parameters. Bakhmeteff (1932b) suggested to impose critical flow conditions to Equation (8). As demonstrated with the aid of the depth-averaged diagram using 2D ideal fluid flow computations the specific energy reaches a minimum value at an overflow crest. Thus it is fully justified to use Equation (8) to find an analytical relationship for the critical depth following Bakhmeteff (1932b). The mathematical condition of an extreme in the specific energy forces E to satisfy the identity

$$\frac{\mathrm{d}E}{\mathrm{d}h} = \frac{\mathrm{d}}{\mathrm{d}h}\left(\Lambda h + \beta \frac{q^2}{2gh^2}\right) = \frac{\mathrm{d}}{\mathrm{d}h}\left(h + \Omega^2 \frac{q^2}{2gh^2}\right) = 0 \tag{10}$$

Equation (10) can be used to find analytically the relationship between the flow at the weir crest, h_{crest}, and the minimum specific energy $E_{\min}$. Developing the last identity of Equation (10) results

$$\frac{q^2}{g h_{crest}^3}\left(\Omega^2 - \Omega h_{crest}\frac{\mathrm{d}\Omega}{\mathrm{d}h}\right) = 1 \tag{11}$$

and, using Equation (9) for find $\mathrm{d}\Omega/\mathrm{d}h$,

$$\frac{h_{crest}}{h_c} = \left[\Omega^2\left(\Omega + \frac{\kappa h_{crest}}{1+\kappa h_{crest}}\right)\right]^{1/3} \tag{12}$$

Equation (12) is the analytical solution for critical curvilinear flow. Introducing Equation (12) into Equation (8) one obtains the value of $E_{\min}$ as

$$\frac{E_{\min}}{h_c} = \frac{h_{crest}}{h_c} + \frac{\Omega^2}{2}\left(\frac{h_{crest}}{h_c}\right)^{-2} \tag{13}$$

The combination of Equations (4) and (13) give the analytical function for C_d based upon critical vortex flow as

$$C_d = \left(\frac{E_{\min}}{h_c}\right)^{-3/2} = \left[\frac{h_{crest}}{h_c} + \frac{\Omega^2}{2}\left(\frac{h_{crest}}{h_c}\right)^{-2}\right]^{-3/2} \tag{14}$$

The procedure to establish the head-discharge relationship of a weir crest is as follows: (a) select a value of h_{crest}/R; (b) compute h_{crest}/h_c from Equation (12); (c) compute $E_{\min}/h_c$ from Equation (13); (d) calculate C_d from Equation (14); (e) find the quotient $h_{crest}/E_{\min}$ dividing Equations (12) and (13); (f) compute $E_{\min}/R$ from the result of step (d) using the value of h_{crest}/R.

Application to flow measurement above circular weirs

Water discharge measurement in open channel systems can be done using weirs (Bos 1976). A particular type of weir of wide interest is the circular weir (Fig. 9a) (Chanson and Montes 1998, Ramamurthy et al. 1992, Ramamurthy and Vo 1993b), where the flow can be considered inviscid and irrotational (Ramamurthy et al. 1994), provided that certain minimum dimensions on R prevail to avoid scale effects (Matthew 1963, 1991). An advantage of the irrotational critical flow theory advocated by Bakhmeteff (1932b) is that C_d depends only of $E_{\min}/R$, such that, for a given R, a unique measurement of $E_{\min}$ yields a prediction of the discharge. This is different from the application of the Dressler equations (e.g. Ramamurthy and Vo 1993a) in which no critical flow condition was invoked to the flow equation. The critical vortex flow theory in circular weirs deserves attention, therefore. A number of experimental data were re-analysed. The results in terms of C_d are plotted in Figure 9b and the curvilinear critical flow depth data in Figure 9c. The predictions of C_d and h_{crest}/h_c using the critical vortex flow theory are depicted in Figure 9. It can be seen that the agreement with experimental data is good up to $E_{\min}/R$=0.7, while the theory could be considered acceptable up to $E_{\min}/R$=1.5, beyond which a free vortex law for the velocity profile ceases to be valid (Ramamurthy and Vo 1993a).

Discussion

The present work extends the use of the classical specific energy equation to study the flow in open channel transitions by introducing a generalized depth-averaged diagram where the pressure is not hydrostatic and the velocity non-uniform. This diagram is based on a depth-averaged form of the Bernoulli equation at any arbitrary section of the channel transition. The development is a generalization of the equation proposed by Chanson (2006) for the minimum specific energy section. The depth-averaged coefficients β and Λ are general definitions for 2D flow and were evaluated for selected test cases.

The characterization of the free surface flow in frictionless open channel transitions requires the determination of the depth-averaged velocity and pressure coefficients, a task so far not done in the literature. Detailed two-dimensional ideal fluid flow computations were used to obtain this information that was introduced in the generalized depth-averaged diagram. The transcritical flow behaviour is first presented rigorously in depth-averaged form using two-dimensional ideal fluid flow data. It is confirmed that critical flow conditions takes place at the overflow section, while subcritical and supercritical flow portions are clearly highlighted. The purpose of this contribution is not to provide an output in the form of depth-averaged coefficients applicable to all flow cases in channel transitions. Rather than this, the purpose of this contribution is to analyze how the general energy equation accounting for non-uniform velocity and non-hydrostatic pressure distributions behaves at channel controls. For this task selected flow cases were solved.

The detailed depth-averaged study supports the assumption of critical flow conditions at an overflow crest (Chanson 2006) and on the horizontal reach preceding a steep chute (Felder and Chanson 2012). The study outcomes are relevant to water discharge measurements in free surface systems, usually conducted by installing weirs of various shapes. In practice, a particular weir design is the circular weir. If scale effects are avoided, the flow above the rounded weir can be simulated using the equations of an inviscid and irrotational flow. Bakhmeteff (1932a) proposed the specific energy equation for hydrostatic pressure and uniform velocity, assumptions that are not accurate at an overflow crest. The generalization to curvilinear flow theory is based upon a free vortex velocity law (Bakhmeteff 1932b) and the results yield the critical flow conditions for curvilinear motion. The analytical development based on this concept was pursued and applied to water discharge measurement using detailed test data.

The present development differ from the works of Sivakumaran et al. (1981, 1983) and Ramamurthy and Vo (1993a), in which the Dressler model was applied for steady-state conditions without resorting to a critical flow theory. Alternatively, critical irrotational flow theory at an overflow crest can be developed using Boussinesq equations (Matthew 1991, Montes 1998). The mathematical apparatus for using Boussinesq equations is however computationally intensive compared to the simple vortex flow theory.

Conclusion

The 'classical' specific energy equation $E=h+U^2/(2g)$ cannot be used to describe the changes of velocity and depth along short channel transitions, despite its use in textbooks based on the so-called specific energy diagram. A generalized depth-averaged diagram is introduced for flows with arbitrary distributions of velocity and pressure, that can be used to properly describe the flow in channel transitions. It is shown that any two-dimensional ideal fluid flow can be depicted in such system of coordinates with generality. For this task a detailed two-dimensional ideal fluid flow solution of typical channel transitions was developed. From the computational data, a detailed description of the depth-averaged channel corrections coefficients, so far not available in the literature, was presented. The ideal fluid flow data was used to present a rigorous picture of the depth-averaged curvilinear flow motion in open channel transitions. The depth-averaged analysis of the motion confirms that critical curvilinear flow conditions take place at an overflow crest and at a horizontal reach preceding a steep chute. The finding was used to pursue a simplified critical irrotational flow theory at overflow sections. From the analytical development, it is proposed an equation for the discharge coefficient of a weir, that is demonstrated to provide accurate water discharge estimates up to $E_{min}/R=0.7$, and may be considered acceptable up to 1.5.

Acknowledgements

The authors acknowledge the inspirational contribution of Dr Sergio Montes (Hobart, Australia) and his original input to the study.

CASTRO-ORGAZ, O., and CHANSON, H. (2014). "Depth-Averaged Specific Energy in Open-Channel Flow and Analytical Solution for Critical Irrotational Flow over Weirs." *Journal of Irrigation and Drainage Engineering*, ASCE, Vol. 140, No. 1, Paper 04013006, 8 pages (DOI: 10.1061/(ASCE)IR.1943-4774.0000666) (ISSN 0733-9437 [Print]; ISSN: 1943-4774 [online]).

Notation

C_d = discharge coefficient (-)

E = specific energy head (m)

$E_{\min}$ = minimum specific energy head (m)

g = acceleration of gravity (m/s^2)

H = total energy head (m)

h = flow depth measured vertically (m)

h_{crest} = crest flow depth (m)

h_c = critical depth for parallel-streamlined flow (m) = $(q^2/g)^{1/3}$

p = pressure (N/m^2)

q = unit discharge (m^2/s)

R = radius of circular-arc (m)

u = velocity in x-direction (m/s)

U = mean flow velocity (m/s) = q/h

v = velocity in y-direction (m/s)

x = horizontal distance (m)

y = vertical elevation (m)

ρ = water density (kg/m^3)

η = vertical coordinate above channel bottom (m)

γ = specific weight of water (N/m^3)

ψ = stream function (m^2/s)

κ = bottom curvature (m^{-1})

β_x = momentum correction coefficient or Boussinesq coefficient (-)

β = kinetic energy correction coefficient (-)

Λ = piezometric pressure correction coefficient (-)

Ω = curvature coefficient (-)

References

Bakhmeteff, B.A. (1932a). *Hydraulics of open channels*. McGraw-Hill, New York.

Bakhmeteff, B.A. (1932b). Discussion to Tests of broad crested weirs. *Trans. ASCE* 96, 423-434.

Bos, M.G. (1976). *Discharge measurement structures*. Publ. 20, Intl. Inst. for Land Reclamation (ILRI), Wageningen NL.

Blau, E. (1963). *Der Abfluss und die hydraulische Energieverteilung über einer Parabelformigem Wehrschwelle*. Mitteilungen der Forschungsanstalt für Schiffahrt, Wasser und Grundbau, Berlin, Heft 7, pp 5-72.

Castro-Orgaz, O. (2013). Potential flow solution for open channel flows and weir crest overflows. *J. Irrig. Drain. Engng*. 139(7), 551-559.

Chanson, H., and Montes, J. S. (1998). Overflow characteristics of circular weirs: effects of inflow conditions. *J. Irrig. Drain. Engng*., 124(3), 152-162.

Chanson, H. (2006). Minimum specific energy and critical flow conditions in open channels. *J. Irrig. Drain. Engng*. 132(5), 498-502.

Dressler, R.F. (1978). New nonlinear shallow flow equations with curvature. *J. Hydr. Res.* 16(3), 205-222.

Fawer, C. (1937). *Etude de quelques écoulements permanents à filets courbes* (Study of certain steady flows with curved streamlines). Thesis, Université de Lausanne. La Concorde, Lausanne, Switzerland [in French].

Felder, S., and Chanson, H. (2012). Free-surface profiles, velocity and pressure distributions on a broad-crested weir: a physical study. *J. Irrig. Drain. Engng*. 138(12), 1068-1074.

CASTRO-ORGAZ, O., and CHANSON, H. (2014). "Depth-Averaged Specific Energy in Open-Channel Flow and Analytical Solution for Critical Irrotational Flow over Weirs." *Journal of Irrigation and Drainage Engineering*, ASCE, Vol. 140, No. 1, Paper 04013006, 8 pages (DOI: 10.1061/(ASCE)IR.1943-4774.0000666) (ISSN 0733-9437 [Print]; ISSN: 1943-4774 [online]).

Hasumi, M. (1931). *Untersuchungen über die Verteilung der hydrostatischen Drücke an Wehrkronen und -Rücken von Überfallwehren infolge des abstürzenden Wassers*. Journal. Dep. Agriculture, Kyushu Imperial University, 3(4), 1-97 [in German].

Henderson, F.M. (1966). *Open channel flow*. McMillan, New York.

Jaeger, C. (1956). *Engineering fluid mechanics*. Blackie and Son, Edinburgh.

Liggett, J.A. (1993). Critical depth, velocity profile and averaging. *J. Irrig. Drain. Engng*. 119(2), 416-422.

Matthew, G. D. (1963). On the influence of curvature, surface tension and viscosity on flow over round-crested weirs. *Proc. ICE* 25, 511-524. Discussion (1964) 28, 557-569.

Matthew, G. D. (1991). Higher order one-dimensional equations of potential flow in open channels. *Proc. ICE* 91(3), 187-201.

Montes, J. S. (1992). A potential flow solution for the free overfall. *Proc. ICE* 96(6), 259-266.

Montes, J. S. (1994). Potential flow solution to the 2D transition from mild to steep slope. *J. Hydr. Engng*. 120(5), 601-621.

Montes, J. S. (1998). *Hydraulics of open channel flow*. ASCE Press, Reston VA.

Rouse, H. (1932). *The distribution of hydraulic energy in weir flow in relation to spillway design*. MS Thesis. MIT, Boston.

Rouse, H. (1938). *Fluid mechanics for hydraulic engineers*. McGraw-Hill, New York.

Ramamurthy, A. S., Vo, N. D., and Vera, G. (1992). Momentum model of flow past a weir. *J. Irrig. Drain. Engng*. 118(6), 988-994.

Ramamurthy, A. S., and Vo, N. D. (1993a). Application of Dressler theory to weir flow. *J. Appl. Mech*., 60, 163-166.

Ramamurthy, A. S., and Vo, N. D. (1993b). Characteristics of circular-crested weirs. *J. Hydr. Engng*., 119(9), 1055-1062.

CASTRO-ORGAZ, O., and CHANSON, H. (2014). "Depth-Averaged Specific Energy in Open-Channel Flow and Analytical Solution for Critical Irrotational Flow over Weirs." *Journal of Irrigation and Drainage Engineering*, ASCE, Vol. 140, No. 1, Paper 04013006, 8 pages (DOI: 10.1061/(ASCE)IR.1943-4774.0000666) (ISSN 0733-9437 [Print]; ISSN: 1943-4774 [online]).

Ramamurthy, A.S., Vo, N. D. and Balachandar, R. (1994). A note on irrotational curvilinear flow past a weir. *J. Fluid Engng*. 116(2), 378-381.

Sivakumaran, N. S., Hosking, R. J., and Tingsanchali, T. (1981). Steady shallow flow over a spillway. *J. Fluid Mech*. 111, 411 -420

Sivakumaran, N. S., Tingsanchali, T., and Hosking, R. J. (1983). Steady shallow flow over curved beds. *J. Fluid Mech*. 128, 469-487.

Thom, A., and Apelt, C. (1961). *Field computations in engineering and physics*. Van Nostrand, London.

Vallentine, H. R. (1969). *Applied Hydrodynamics*. Butterworths, London.

Vo, N.D. (1992). *Characteristics of curvilinear flow past circular-crested weirs*. Ph.D. Thesis. Concordia Univ., Canada.

List of figures

Figure1
Click here to download high resolution image

Figure2
Click here to download high resolution image

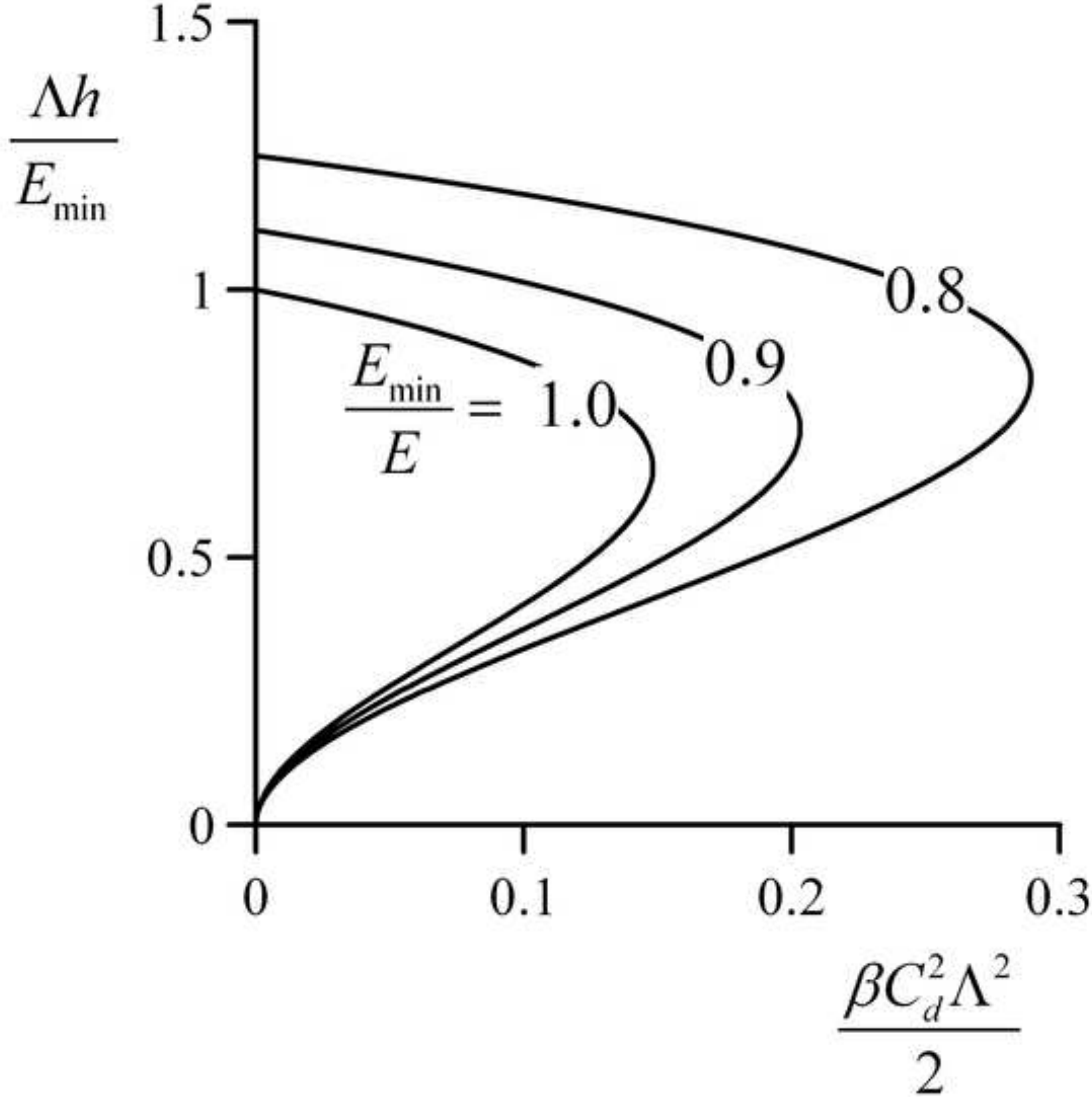

Figure3
Click here to download high resolution image

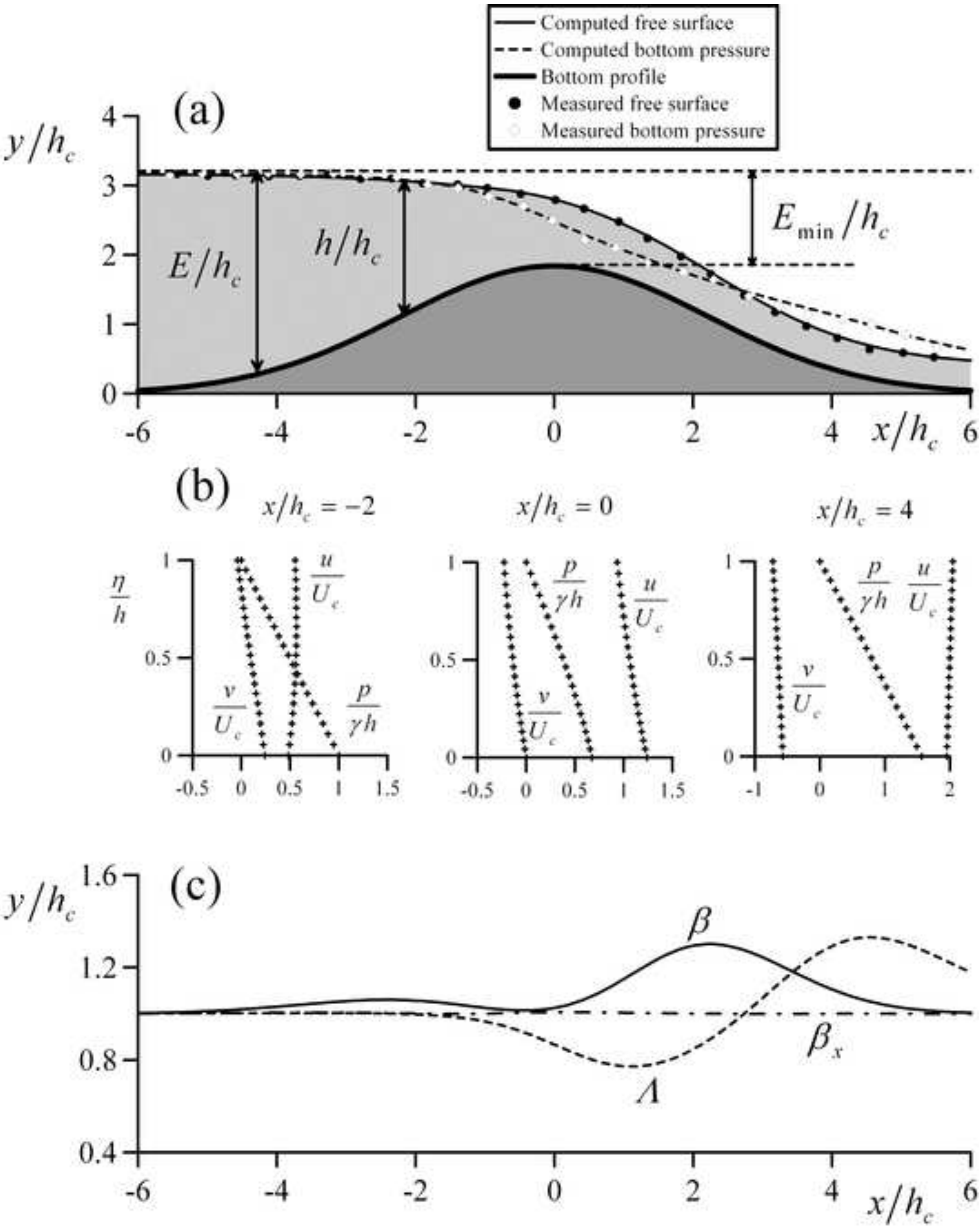

Figure4

Click here to download high resolution image

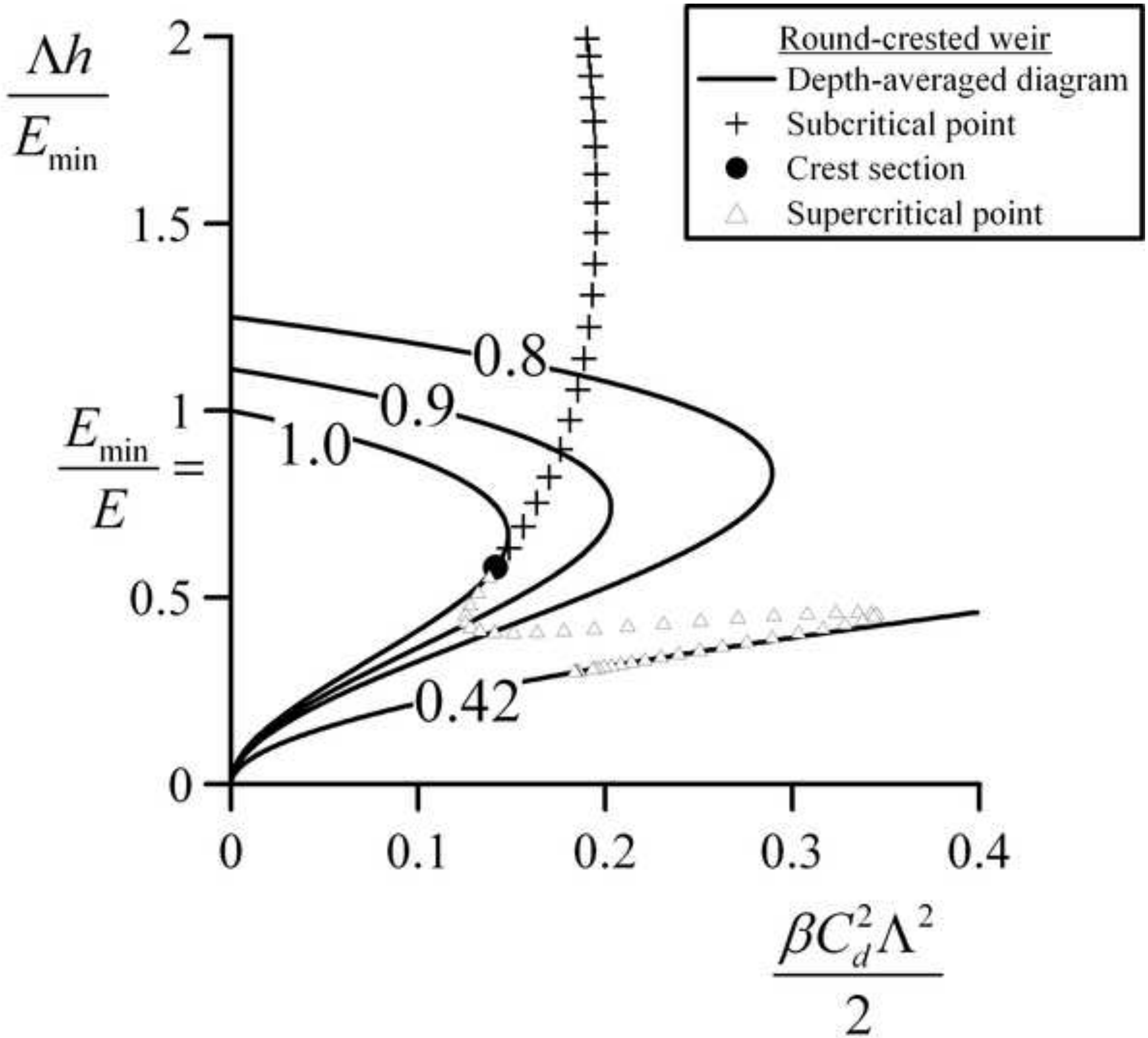

Figure5

Click here to download high resolution image

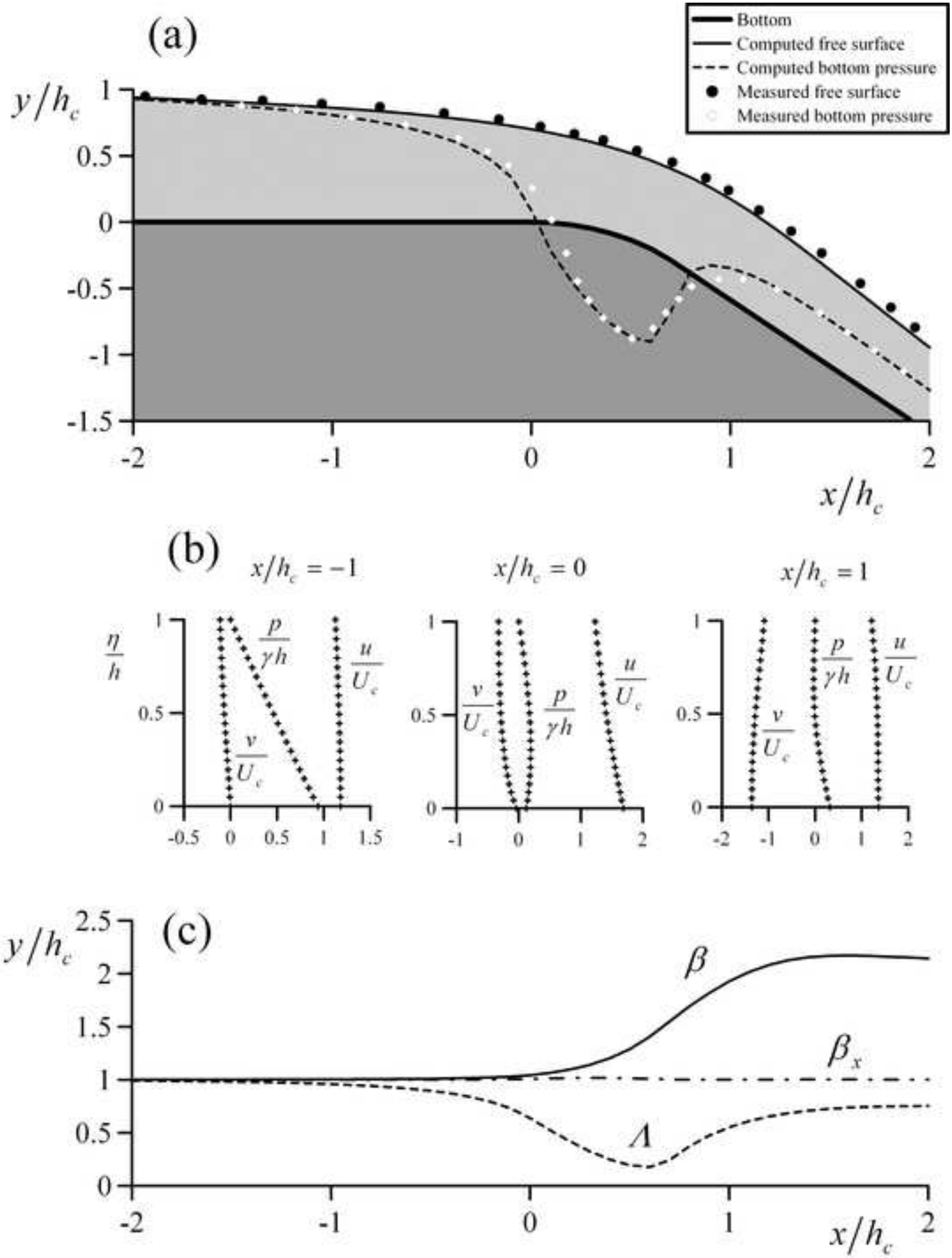

Figure6
Click here to download high resolution image

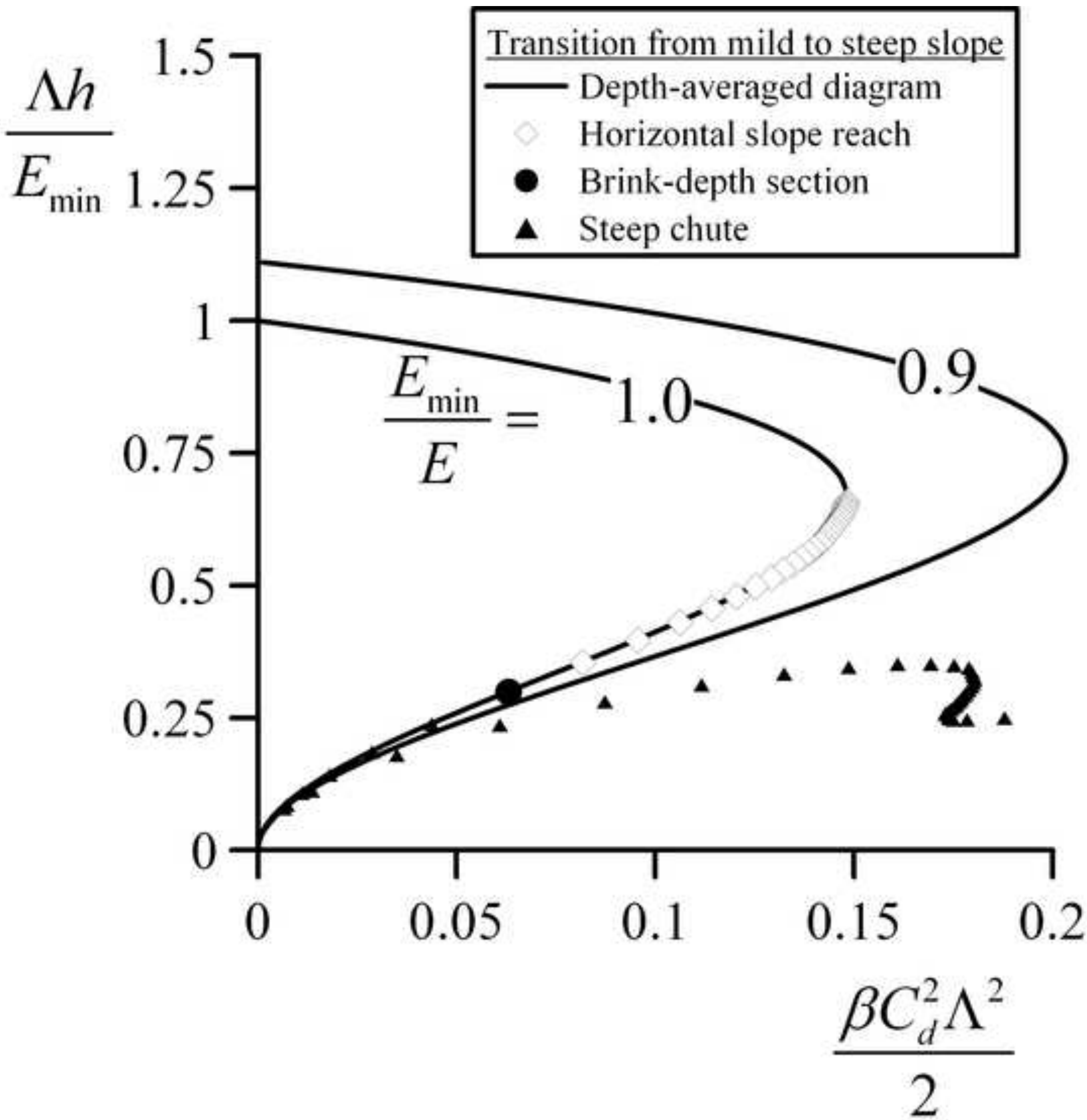

Figure7
Click here to download high resolution image

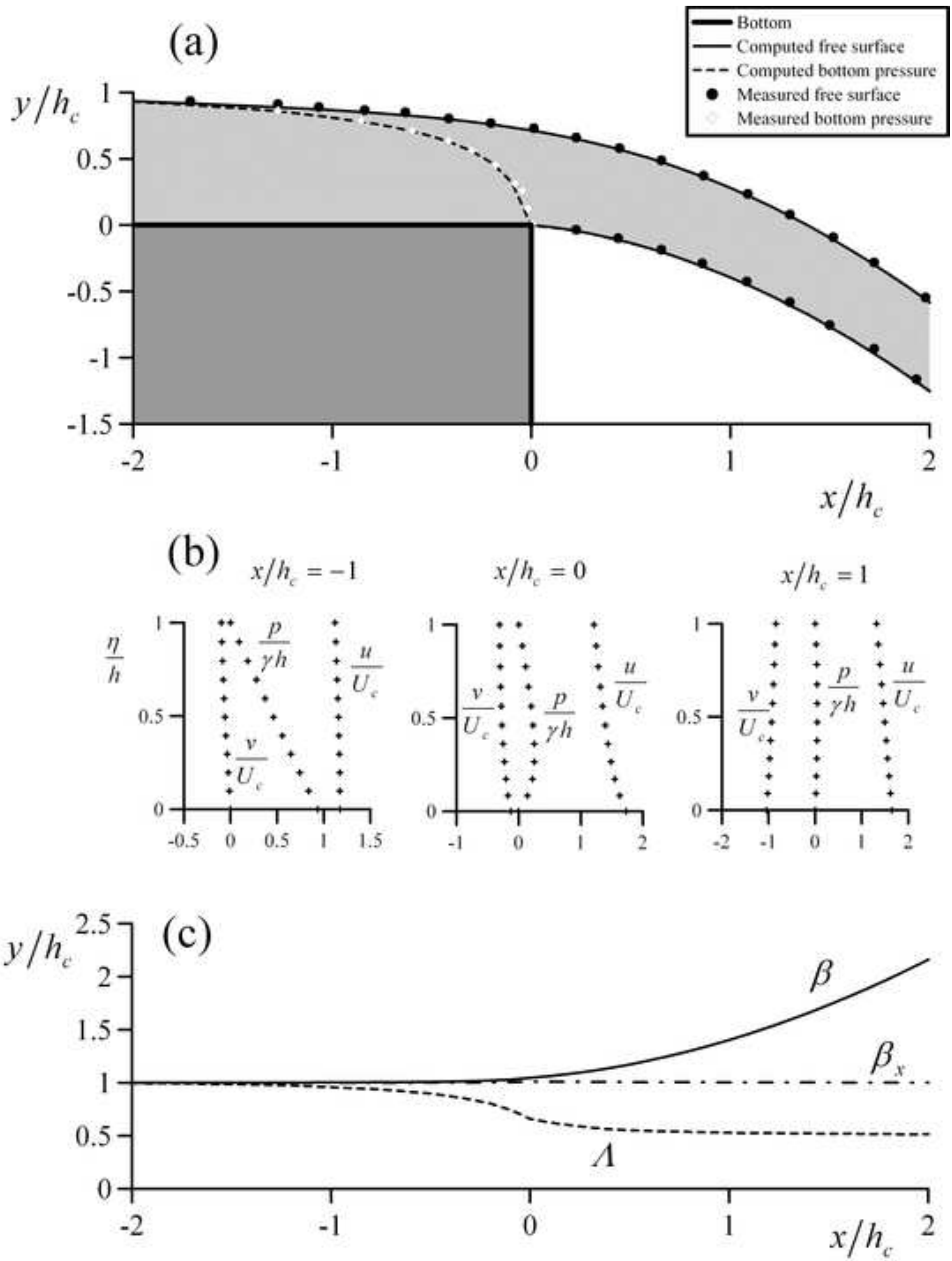

Figure8
Click here to download high resolution image

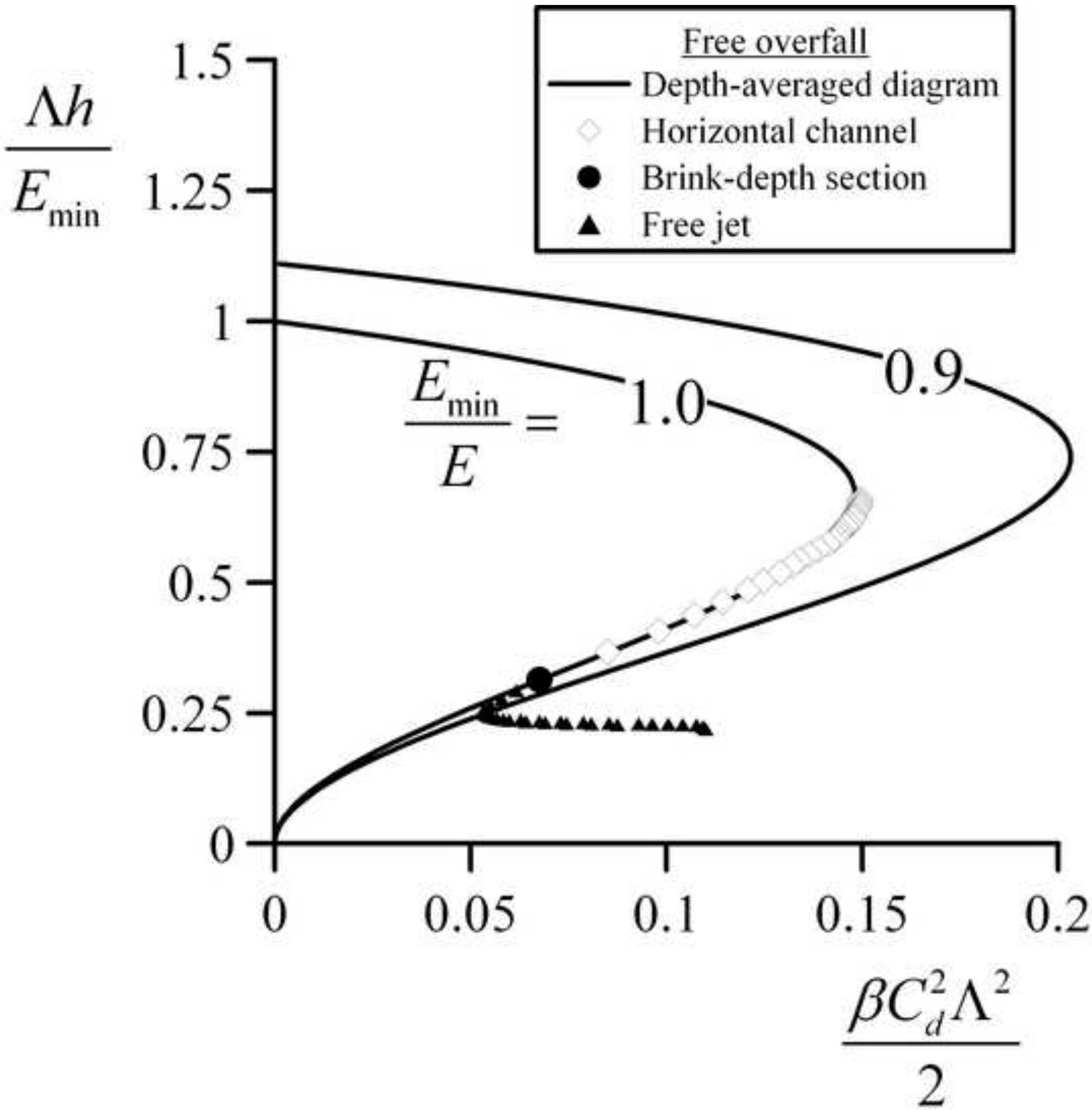

Figure9
Click here to download high resolution image